Supporting Information

Structural basis for the binding of SNAREs to the multisubunit tethering complex Dsl1

Sophie M. Travis, Kevin DAmico, I-Mei Yu, Safraz Hamid, Gabriel Ramirez-Arellano, Philip D. Jeffrey, and Frederick M. Hughson

Contents

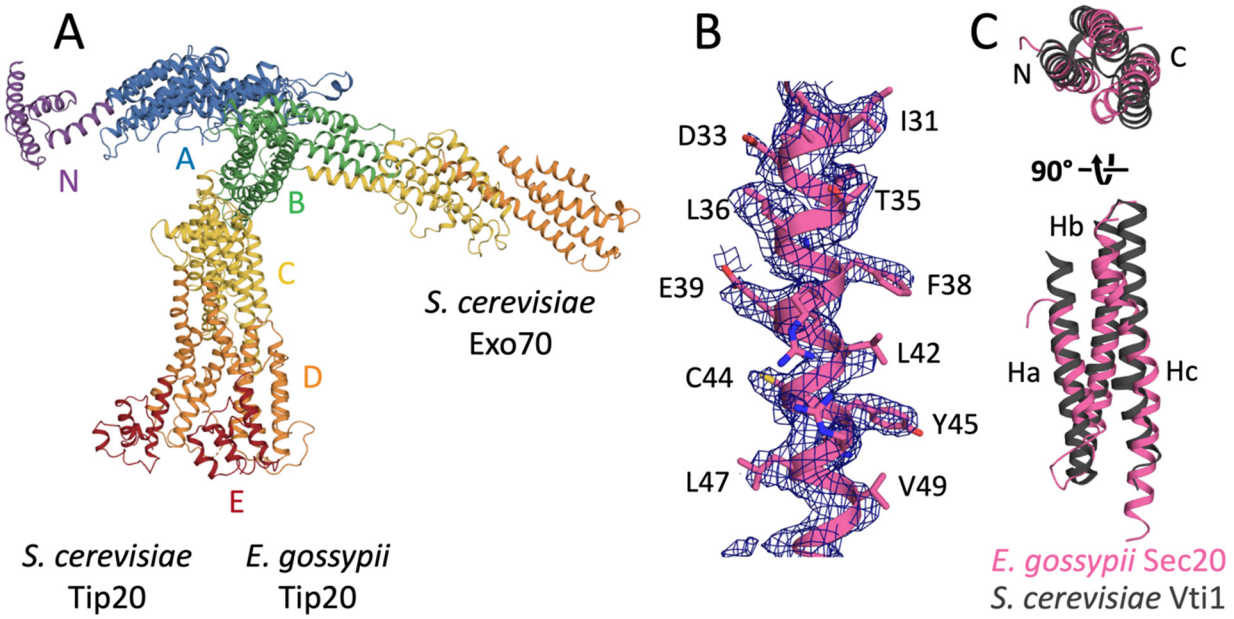

Figure S1. Comparative analysis of *E. gossypii* Tip20 and Sec20 structures. *A, E. gossypii* and *S. cerevisiae* Tip20 (3FHN, chain A) superimpose with an RMSD of 2.9 Å over 394 residues. The major difference between the two structures is the different relative orientation of domains B and C. *S. cerevisiae* Exo70 (2PFV) adopts a much more linear configuration. The three proteins are shown aligned on domain A. *B,* Representative electron density for *E. gossypii* Sec20 (pink), showing side chain assignments. The composite omit 2Fo-Fc map (dark blue mesh) is contoured at 1σ. *C, E. gossypii* $Sec20_{NTD}$ (pink) resembles *S. cerevisiae* Vti1 (3ONJ, gray), superimposing with an RMSD of 2.3 Å over 78 residues of the structure.

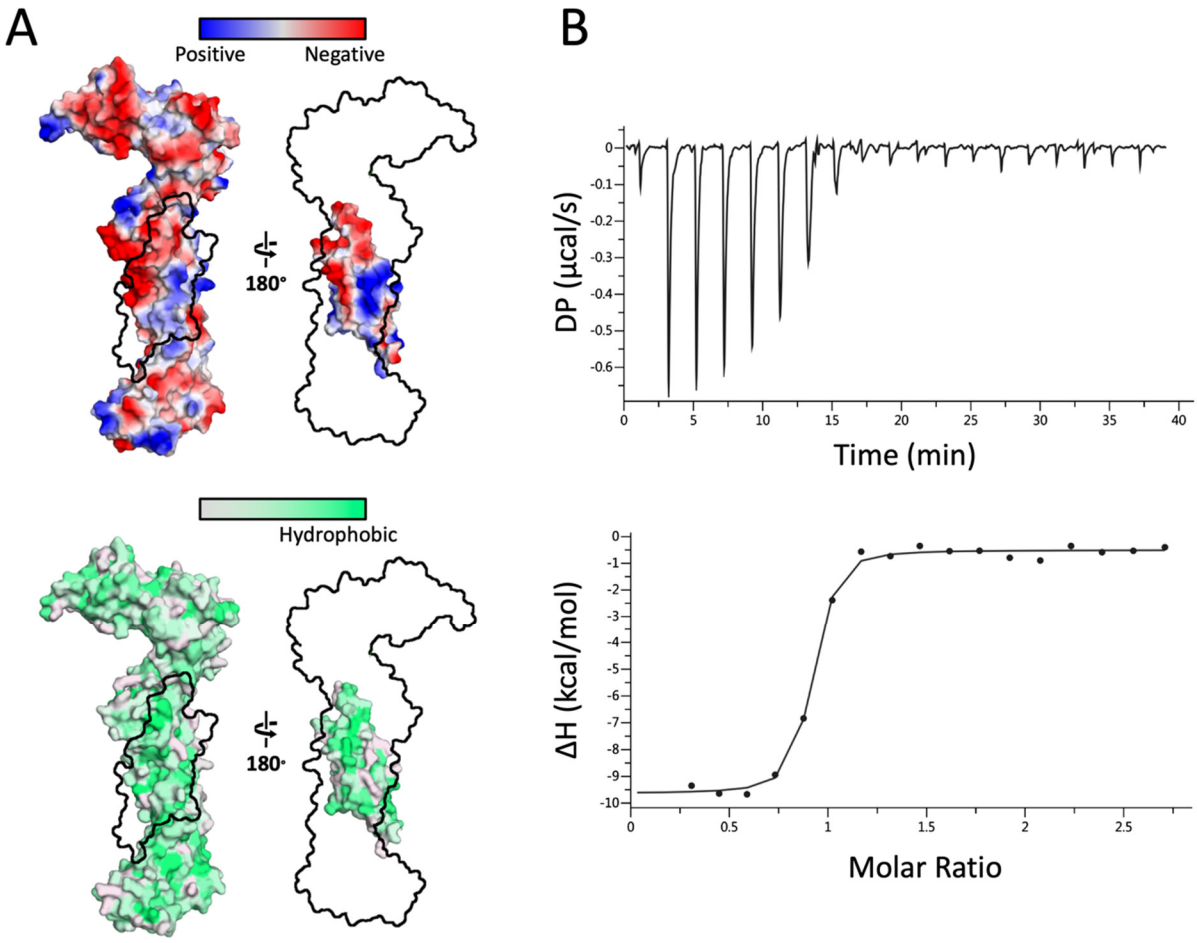

Figure S2. Properties of the *E. gossypii* Tip20•Sec20 complex. *A,* The protein:protein interface lacks obvious distinguishing features in terms of surface electrostatic potential (top) or hydrophobicity (bottom). *B,* Isothermal titration calorimetry data for MBP-Sec20$_{1\text{-}136}$ and Tip20; see Table S2.

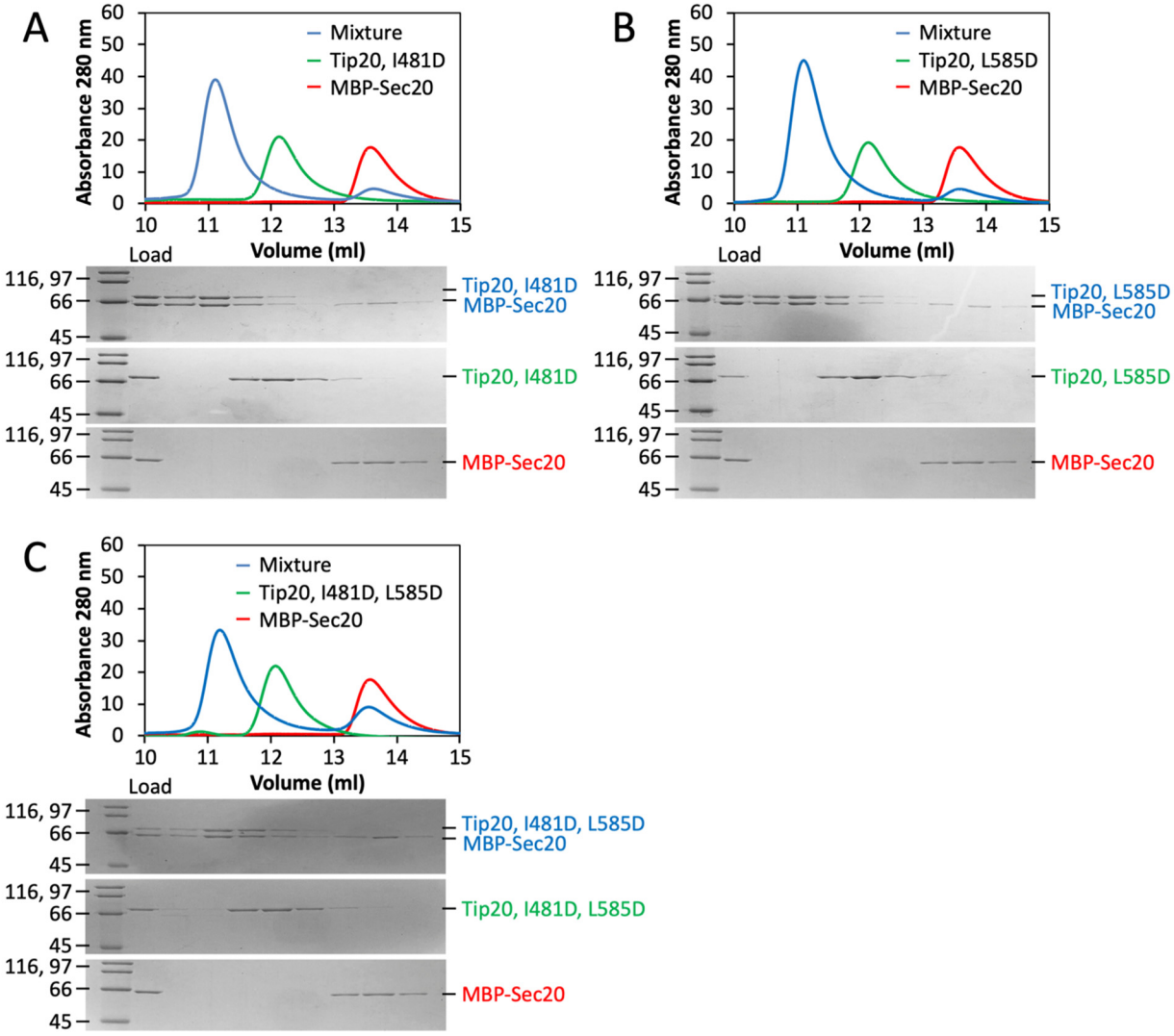

Figure S3. *S. cerevisiae* Tip20 mutants minimally affect binding as judged by size exclusion chromatography. *A-C,* Replacing *S. cerevisiae* Tip20 Ile-481, Leu-585, or both with aspartate had little effect on complex formation. The data presented for MBP-Sec20 alone in (*A-C*) are identical to that in Figure 3*A*.

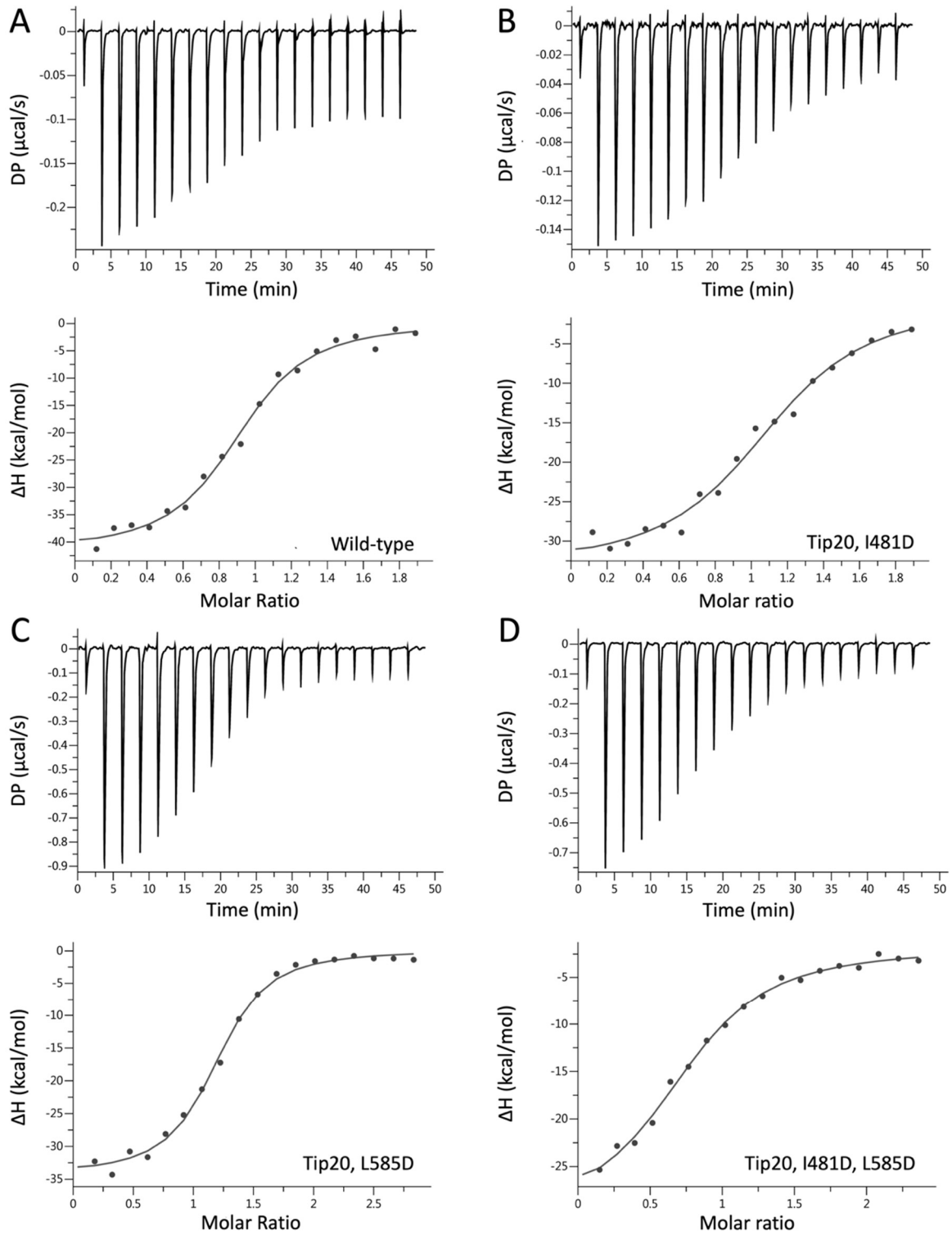

Figure S4. Structure-based mutations destabilize the *S. cerevisiae* Tip20•Sec20$_{1\text{-}174}$ complex. *A-D,* Isothermal titration calorimetry data for Sec20$_{1\text{-}174}$ and the indicated Tip20 mutants; see Table S2.

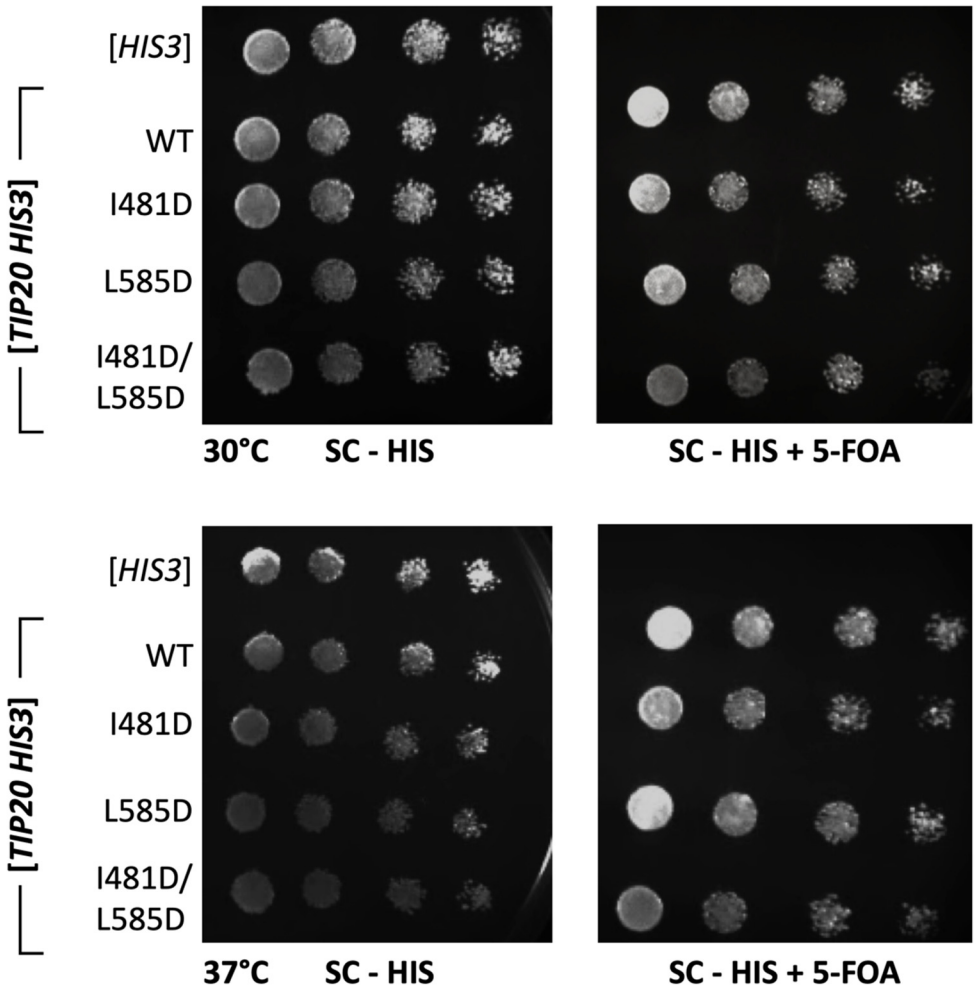

Figure S5. *S. cerevisiae* Tip20 interface mutants are viable. As in Figure 4, mutant alleles of *S. cerevisiae* Tip20, linked to His3, were tested for viability upon counterselection against a wild-type copy of Tip20, linked to Ura3. Although an empty His3 plasmid was not able to support viability, all alleles of Tip20 tested were viable, even at elevated temperature.

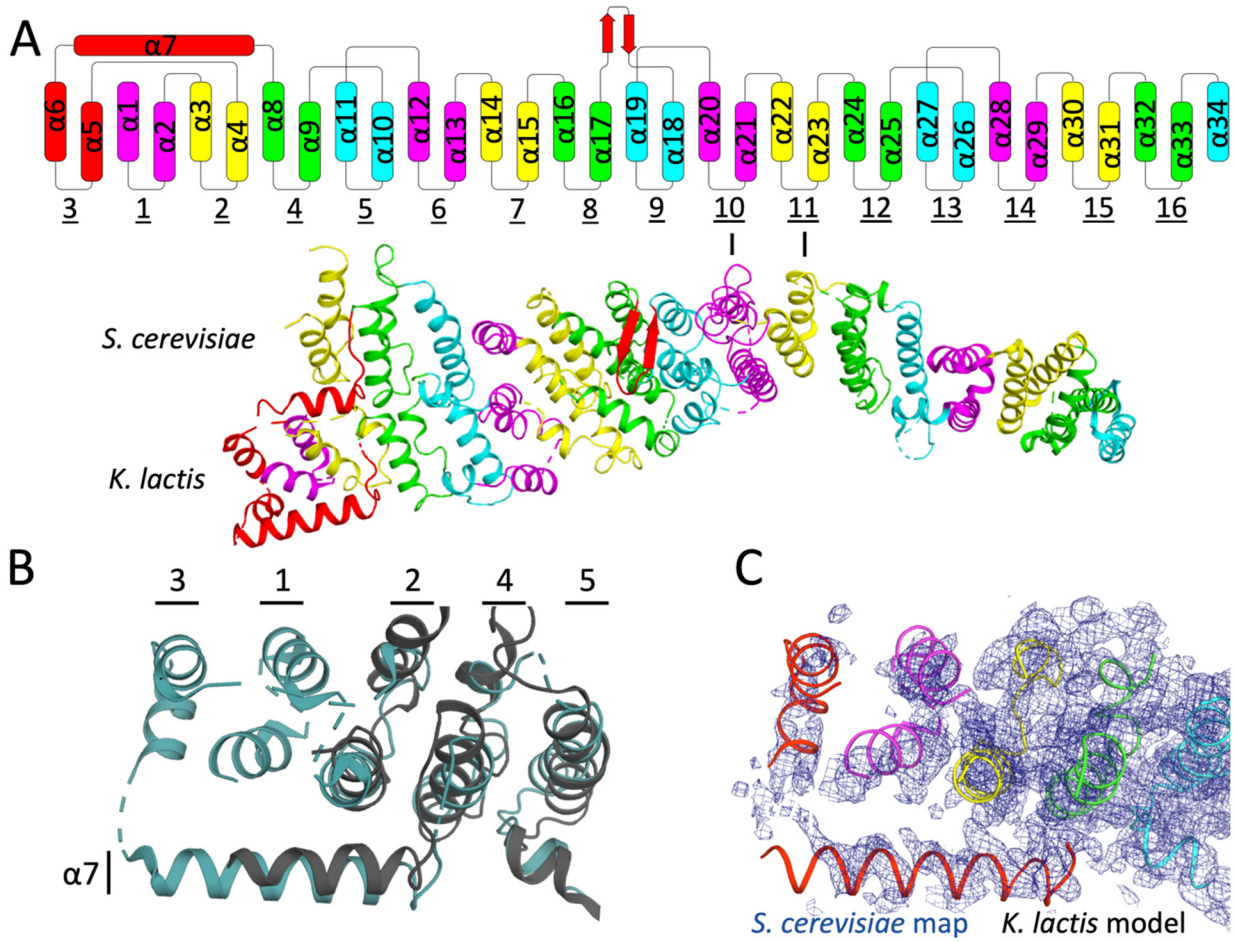

Figure S6. Additional N-terminal regions modeled for *K. lactis* Sec39. *A,* Above, topology of Sec39, with color-coding to illustrate the correspondence between individual α-helices and hairpins. Below, *S. cerevisiae* and *K. lactis* Sec39 superimpose with an RMSD of 3.7 Å over 436 residues. Superimposition at the C-terminus shows that the two structures differ primarily due to bending between layers 10 and 11 (indicated). *B,* Four additional helices were modeled at the N-terminus of *K. lactis* Sec39 (cyan), representing hairpins 1 and 3. In addition, the N-terminus of α7 was extended relative to *S. cerevisiae* Sec39 (3K8P, gray). The two structures are superimposed at the N-terminus. *C,* Contoured at 1 σ, the *S. cerevisiae* 2Fo-Fc map (3K8P, blue mesh) contains weak density, not previously interpreted, corresponding to hairpins 1 and 3 as modeled in the *K. lactis* structure.

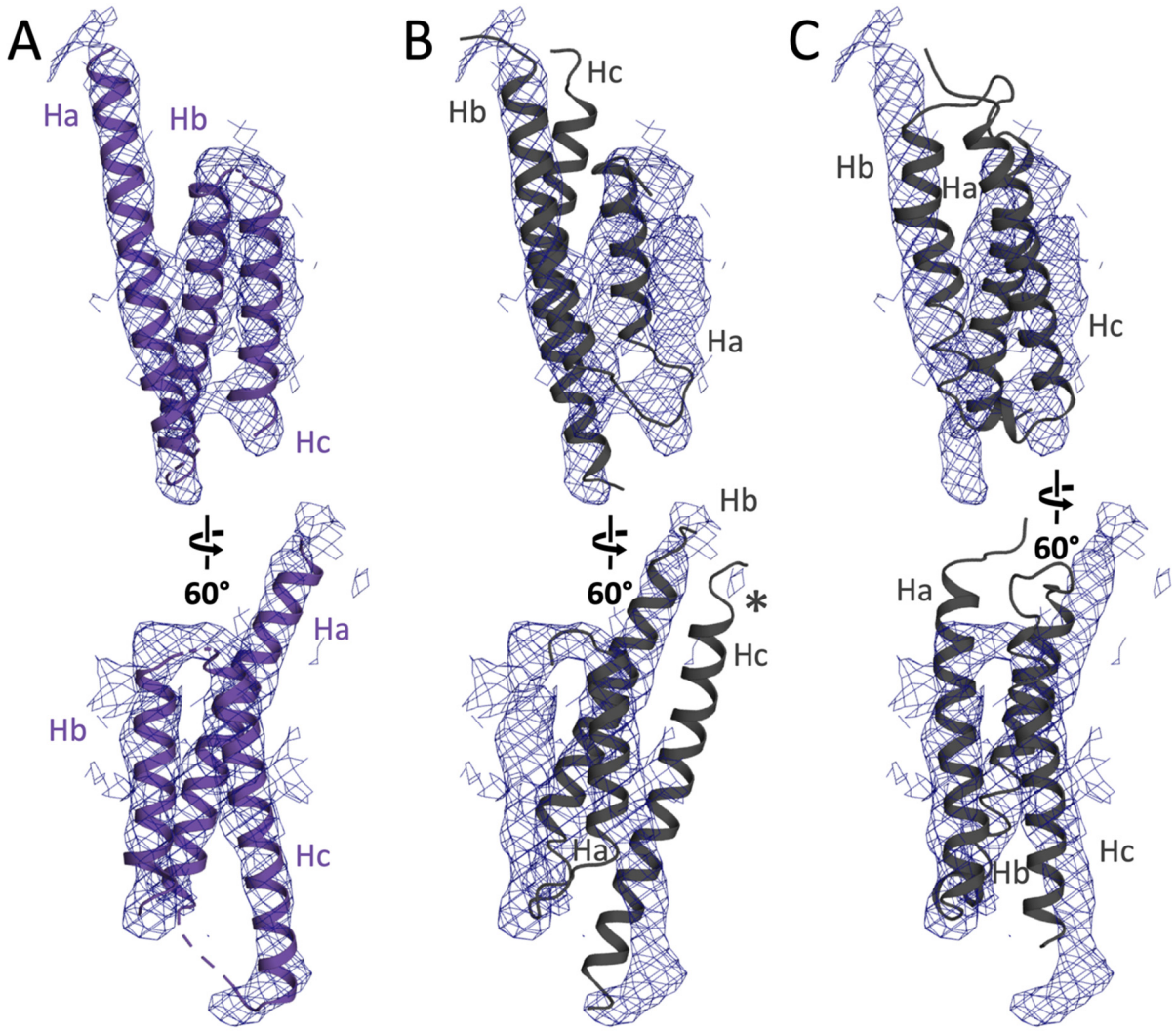

Figure S7. Electron density for *K. lactis* Use1 is consistent with an Habc domain topology. *A,* Contoured at 1 σ, the *K. lactis* 2Fo-Fc SNARE omit map (blue mesh) contains density for three α-helices, here modeled based on the top scoring molecular replacement solution, *S. cerevisiae* Vti1 (3ONJ, gray). *B,* An alternative molecular replacement solution, obtained by using *E. gossypii* Sec20 as a search model, failed to occupy all three helical densities. The starred helix instead clashes with hairpins 1 and 3 of Sec39. *C,* A second alternative molecular replacement solution, obtained by using *S. cerevisiae* Vam3 (1HS7) as a search model, failed to recapitulate inter-helix connectivities present in the electron density map. See also Table S3.

Figure S8. Secondary structure prediction suggests that the N-terminal domain of Use1 is α-helical. Secondary structure prediction (61) identified three putative α-helices in the N-terminal domain of *K. lactis* Use1. Because the first helix in the sequence is not conserved among some orthologues, including *S. cerevisiae*, it is possible that the long Ha helix observed in Use1 comprises the first two predicted helices. Sequence conservation is shown in purple.

Table S1. Summary of crystallographic parameters.

	E. gossypii $Tip20_{A-E}$•$Sec20_{NTD}$ (PDB 6WC3)	*K. lactis* $Sec39$•$Use1_{NTD}$•$Dsl1_{C-E}$ (PDB 6WC4)	
Data collection			
Beamline	NSLS-II AMX	NSLS-II FMX	
Wavelength (Å)	0.97930	0.97932	
Space group	$P6_222$	C121	
Cell dimensions			
a, b, c (Å)	133.3, 133.3, 288.5	240.8, 87.9, 161.4	
α, β, γ (°)	90.0, 90.0, 120.0	90.0, 196.6, 90.0	
		Isotropic	**Anisotropic**[b]
Resolution (Å)[a]	28.12-3.20 (3.32-3.20)	29.30-6.56 (6.79-6.56)	29.60-5.73 (6.65-5.73)
Total reflections	665895	42694	47884
Unique reflections	25534	6268	7053
Completeness (%)[a]	99.1 (93.5)	97.5 (90.3)	89.5 (55.5)
Multiplicity [a]	26.1 (22.7)	6.8 (6.2)	6.8 (6.4)
R_{merge} (%)[a]	13.1 (106)	9.8 (165)	11.5 (181)
R_{meas} (%)[a]	13.4 (109)	10.6 (180)	13.5 (217)
$\langle I/\sigma_I \rangle$ [a]	27.6 (3.5)	11.4 (1.0)	10.7 (1.1)
$CC_{1/2}$ [a]	1.000 (0.896)	0.998 (0.344)	0.997 (0.319)
Refinement			
Resolution (Å)	28.12-3.20		29.60-5.73
No. reflections	25522		7034
R_{work}/R_{free} (%)	0.210/0.248		0.276/0.321
No. atoms	5482		6126
Protein	5482		6126
Water	0		0
Average B-factor (Å^2)	79.5		398
RMSD			
Bond lengths (Å)	0.005		0.009
Bond angles (°)	1.08		1.16
Clashscore	6.69		9.9
Ramachandran			
Favored	95.8		95.1
Allowed	4.2		4.4
Outliers (%)	0		0.5

[a]Values in parentheses are for the highest resolution shell.
[b]An elliptical resolution cut-off was applied to the data using the STARANISO server. Values listed are first using a traditional spherical cut-off and second extended using an elliptical cut-off. STARANISO identified an isotropic cut-off resolution limit of 6.73 Å and an elliptical worst-diffraction limit of 7.15 Å.

Table S2. Isothermal titration calorimetry fit parameters of *S. cerevisiae* Tip20 mutants.

Cell	Syringe	N	K_D (nM)	ΔH (kcal/mol)	ΔG (kcal/mol)	-TΔS (kcal/mol)
E. gossypii Tip20 (30 μM)	*E. gossypii* MBP-$Sec20_{1-136}$ (420 μM)	0.86 ±0.01[a]	88 ± 20[a]	-9.1 ± 0.2[a]	-9.6	-0.51
S. cerevisiae Tip20 (2.5 μM)	*S. cerevisiae* $Sec20_{1-174}$ (25 μM)	0.90 ±0.02[a]	110 ± 30[a]	-42 ± 2[a]	-9.5	32
S. cerevisiae $Tip20_{I481D}$ (2.5 μM)	*S. cerevisiae* $Sec20_{1-174}$ (25 μM)	1.11 ±0.05[a]	190 ± 60[a]	-33 ± 3[a]	-9.2	24
S. cerevisiae $Tip20_{L585D}$ (10 μM)	*S. cerevisiae* $Sec20_{1-174}$ (150 μM)	1.16 ±0.02[a]	400 ± 70[a]	-34 ± 1[a]	-8.7	26
S. cerevisiae $Tip20_{I481D/L585D}$ (12 μM)	*S. cerevisiae* $Sec20_{1-174}$ (150 μM)	0.78 ±0.02[a]	1700 ± 400[a]	-29 ± 2[a]	-7.9	21

[a]Errors reported are fit errors.

Table S3. Alternative Use1 Habc domain molecular replacement solutions.

PDB code	Protein	Type	Species	eLLG[a]	Solution[b]
3ONJ	Vti1	Qb-SNARE	*S. cerevisiae*	637.7	A
6WC3	Sec20	Qb-SNARE	*E. gossypii*	634.3	B
1VCS	Vti1a	Qb-SNARE	*M. musculus*	631.4	B
4J2C	Stx6	Qc-SNARE	*H. sapiens*	630.1	B
2C5K	Tlg1	Qc-SNARE	*S. cerevisiae*	624.1	B
2V8S	Vti1b	Qb-SNARE	*H. sapiens*	623.5	B
1HS7	Vam3	Qa-SNARE	*S. cerevisiae*	619.9	C
1FIO	Sso1	Qa-SNARE	*S. cerevisiae*	604.0	C
1LVF	Stx6	Qc-SNARE	*R. norvegicus*	582.4	B

[a]Final expected log likelihood gain calculated by Phaser, a metric to assess quality of molecular replacement solution that takes into account both resolution and predicted homology to search model.
[b]The solutions clustered into three types. An example of each solution type is depicted in Figure S7, in the corresponding panels *A*-*C*.